

FINITE ELEMENT ANALYSES OF RAILROAD TANK CAR HEAD IMPACTS

Y.H. Tang

Volpe National Transportation Systems Center
Cambridge, Massachusetts, USA

H. Yu

Chenga Advanced Solutions & Engineering, LLC
Cambridge, Massachusetts, USA

J.E. Gordon

Volpe National Transportation Systems Center
Cambridge, Massachusetts, USA

D.Y. Jeong

Volpe National Transportation Systems Center
Cambridge, Massachusetts, USA

ABSTRACT

This paper describes engineering analyses of a railroad tank car impacted at its head by a rigid punch. This type of collision, referred to as a head impact, is examined using dynamic, nonlinear finite element analysis (FEA). Commercial software packages ABAQUS and LS-DYNA are used to carry out the nonlinear FEA. The sloshing response of fluid and coupled dynamic behavior between the fluid inside the tank car and the tank structure are characterized in the model using both Lagrangian and Eulerian mesh formulations. The analyses are applied to examine the structural behavior of railroad tank cars under a generalized head impact scenario. Structural behavior is calculated in terms of forces, deformations, and puncture resistance. Results from the two finite element codes are compared to verify this methodology for head impacts. In addition, FEA results are compared to those from a semi-empirical method.

INTRODUCTION

Recent train derailments involving the release of hazardous materials (hazmat) have prompted renewed focus on the structural integrity of tank cars during accidents [1-3]. Consequently, the industry began efforts to develop improved designs while the government initiated research to develop performance standards for tank cars carrying hazmat [4].

The Volpe National Transportation Systems Center (Volpe Center) provides technical support to the Federal Railroad Administration (FRA) by conducting and managing research to evaluate the structural integrity and crashworthiness of tank cars carrying hazmat. Prior to these recent accidents, the

objective of FRA/Volpe Center research was to maintain tank integrity under normal operating conditions (e.g., metal fatigue and damage tolerance). More recently, the focus of the research has shifted to also maintain tank integrity under rare and extreme circumstances such as impact loading during accidents. Previous research has been conducted by the Volpe Center to examine tank car impacts to the head [5] and the side or shell [6, 7] of tank cars. Such failures occur from collisions with objects such as couplers and wheels from adjacent cars, broken rails, etc.

In the 1970s, a semi-empirical method to examine tank car head puncture was developed through the Railroad Tank Car Safety Research and Test Project [8].¹ This method included equations to calculate puncture velocity, which is the impact velocity at which puncture of the commodity tank is expected to occur. Subsequently the semi-empirical method was modified to account for the presence of jackets and head shields [9]. Correlations with data from additional sources [10] and with engineering analyses [11] indicate that the semi-empirical approach to predict puncture velocity gives reasonable but conservative estimates. That is, puncture is expected to occur at velocities greater than the calculated value.

FEA offers an alternative approach to the semi-empirical approach, which can reduce conservatism since it provides more realistic modeling of impacts. Results from FEA models were presented previously in reference [5], but the effects of

¹ This project is now co-sponsored by the Railway Supply Institute (RSI) and the Association of American Railroads (AAR).

fluid-structure interaction and material failure were not included. Over time, the capabilities of state-of-the-art FEA software have progressed to readily implement these effects. A methodology using commercial FEA software was recently developed to examine shell impacts accounting for fluid-structure interaction and material failure. In this paper, the FEA methodology for shell impacts is adapted to examine head impacts in a consistent and analogous manner.

This paper describes dynamic, nonlinear finite element models to examine the structural behavior of tank cars under a generalized head impact scenario. These models were developed using commercial finite element codes ABAQUS [12] and LS-DYNA [13], which were used previously in the methodology developed for shell impacts. Structural behavior is examined in terms of impact force as a function of indentation. Force-indentation characteristics are examined for different tank car configurations. These configurations include a baseline conventional tank car designed to carry liquid chlorine, a baseline tank with a head shield, and a baseline tank with increased thickness and a head shield. In addition, puncture velocities are calculated for these different configurations. FEA results are compared to those from the semi-empirical method.

Confidence and credibility in the FEA models for shell impacts was achieved through a process of verification and validation.² Verification was conducted by comparing results from both solvers with each other and with known solutions for static loading. Validation for shell impacts was accomplished through comparisons with data obtained from full-scale tests that were performed at the Transportation Technology Center in Pueblo, Colorado [6]. In this paper, verification of the FEA models for generalized head impacts is conducted by comparing results from both solvers with each other.

FINITE ELEMENT ANALYSIS

Finite element models are developed to examine the deformation and failure of railroad tank cars due to head impacts. The idealized impact scenario is a tank car moving into a fixed and rigid indenter at a given impact velocity. Figure 1 shows a schematic of the FEA model for the idealized head impact scenario. The impact location on the tank head is 34 inches below the center of the head. Unless specified otherwise, the dimensions of the indenter face are 6 inches by 6 inches with 0.5-inch edge radii.

All tank cars models are half-symmetric about the longitudinal center plane with 10.6 percent outage³ and an internal pressure of 100 psi. The elliptical shape of the end caps is created with an aspect ratio of 2. An 11-gage (0.119-

² In the present context, verification refers to the process in ensuring that the mathematics are being modeled correctly. Validation refers to the process in determining whether physics are being modeled correctly [14].

³ Outage is the unfilled volume of the tank. Therefore 10.6 percent outage represents a tank that is slightly less than 90 percent full.

This material is declared a work of the U.S. Government and is not subject to copyright protection in the United States. Approved for public release; distribution is unlimited.

inch thick) jacket is modeled with a 4-inch separation to account for the presence of insulation and thermal protection between the commodity tank and the jacket.

The FEA models do not include tank car components such as the manway, body bolsters, draft sills, and safety appliances. Despite these simplifications, the computational times for the FEA models are extensive because the models account for the following physical characteristics of deformable bodies under impact loading: (1) structural dynamics, (2) elastic-plastic material behavior with large deformations, (3) fluid-structure interaction, and (4) material failure.

FEA is well established as a computational tool to model structural dynamics to simulate structure movement with respect to time under prescribed loads.

Both ABAQUS and LS-DYNA include standard constitutive models for elastic-plastic stress-strain behavior with large deformation. The elastic-plastic material behavior is modeled using Ramberg-Osgood equation for strain as a function of stress.

$$\varepsilon = \frac{\sigma}{E} + \left(\frac{\sigma}{K} \right)^n \quad (1)$$

where ε is the strain, σ is the stress, n and K are material constants and E is the modulus of elasticity. Table 1 lists constants and mechanical properties of the tank car steels that are used in the FEA models described in this paper. In current tank car construction, the commodity tank is nominally made with normalized TC-128B steel. The properties listed in the table for TC-128B correspond to tensile measurements performed on tank car that punctured in a full-scale shell impact test [6]. Outer jackets are typically made with A1011 steel. Properties for A1011 are available from the Internet. Current practice requires that commodity tanks greater than 1 inch thick must be built with steels other than TC-128B. In these cases, A516-70 steel is used in the FEA models. The properties listed for this particular steel are obtained from reference [15].

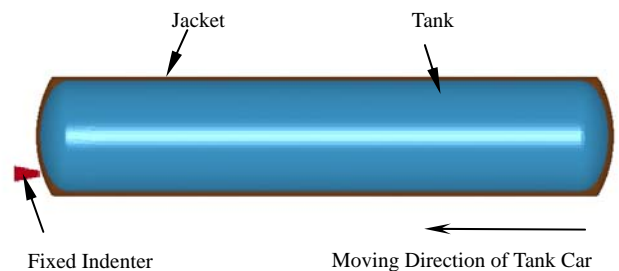


Figure 1: Schematic of FEA Simulation

Table 1: FEM Constants and Mechanical Properties

	TC-128B	A1011	A516-70
Modulus of elasticity, E (ksi)	31,650	29,000	30,000
Hardening exponent, n	11.17	9.00	10.64
R-O Constant, K (ksi)	96.04	59.85	89.69
Yield strength (ksi)	55.05	30	50
Tensile strength (ksi)	83.05	50	70

When there is fluid inside the tank, both the fluid and the tank move and exert forces upon one another during impact. Different mesh representations are used in the FEA models to account for this fluid-structure interaction behavior. Specifically, Lagrangian and Eulerian mesh formulations are used. In the Lagrangian fluid formulation, the nodes of the mesh representing the fluid follow the material of the structure as it deforms. This formulation is used in both the ABAQUS and LS-DYNA simulations discussed in this paper. An Eulerian mesh is fixed in space and tracks the material movement inside the structural Lagrangian mesh of the tank. The Eulerian formulation is implemented using LS-DYNA. Previous research on tank car shell impacts [6, 7] indicated that the Eulerian mesh provided a more accurate representation of fluid-structure interaction than the Lagrangian mesh when compared to test data.

ABAQUS Implementation

The ABAQUS simulations discussed in this paper are performed with the explicit dynamics program ABAQUS/Explicit Version 6.7-1 [12].

The tank car assembly of the ABAQUS model includes the deformable tank, jacket and fluid components. Two planar rigid bodies are also placed in front and rear positions under the tank car assembly to simulate some effects of rail car wheels. These front and rear “wheels” are coupled in rigid body motion with selected front and rear element sets, respectively, in the bottom of the tank car assembly. A rigid “floor” prevents the “wheels,” as well as the tank car assembly, from moving downward. The tank car assembly and the “wheels” are assigned an initial horizontal speed toward a rigid indenter that is constrained in all degrees of freedom.

Shell elements used in conjunction with elastic-plastic constitutive relations are accurate and efficient in simulating the force-deformation behavior of the tank structure without failure. In modeling failure, however, solid elements in the vicinity of impact are needed to produce accurate results in simulating progressive damage and fracture behavior. A small sub-domain at and around the location of impact is modeled with solid elements, whereas the remaining tank structure is modeled with shell elements. This computational strategy is implemented using the solid-to-shell coupling capability within ABAQUS [12]. Figure 2 shows a typical solid-to-shell coupling mesh in the model.

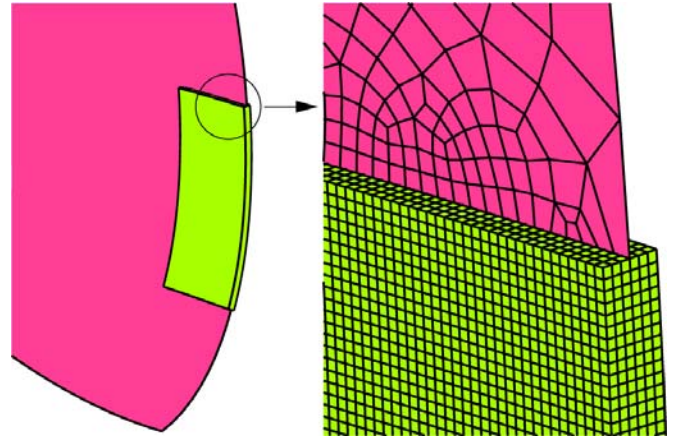


Figure 2: Close-Up View of a Typical Solid-to-Shell Coupling Mesh

Material failure is implemented in ABAQUS with a standard constitutive material model and a resident failure initiation and progression model based on the general state of stress and strain softening. Failure is assumed to initiate when loading conditions induce effective plastic strains above a threshold value that depends on the general state of stress in terms of a quantity called stress triaxiality. Stress triaxiality is the ratio of mean stress to the effective or von Mises equivalent stress. Figure 3 shows a schematic of the effective plastic strain to initiate failure, ϵ_i as a function of stress triaxiality, η . Moreover, this envelope is referred to as the Bao-Wierzbicki (B-W) criterion [16]. The schematic indicates that the B-W failure initiation envelope consists of three regions, each representing a different mode of failure. Region I consists of high positive values of stress triaxiality which promotes nucleation, growth, and coalescence of voids leading to ductile fracture. Region III consists of negative values of stress triaxiality which represent shear fracture due to shear band localization. Region II comprises positive but low values of stress triaxiality, and represents mixed fracture.

Once failure initiates, damage is assumed to progress in the form of strain softening. The resident failure model in ABAQUS has the option to specify linear or exponential strain softening. In the present implementation, linear strain softening is assumed. Figure 4 illustrates this concept in which the stress-strain behavior of a material element exhibits a linear decrease in stress with increasing strain beyond ϵ_i . The implementation of progressive damage in ABAQUS is actually in the form of a stress-displacement where the effective plastic strain is multiplied by a characteristic length.⁴

⁴ For shell and two-dimensional elements, this characteristic length is the square root of the integration point area; for three-dimensional elements, it is the cube root of the integration point volume. The definition of the characteristic length indicates that some mesh dependency is expected when elements have poor aspect ratios.

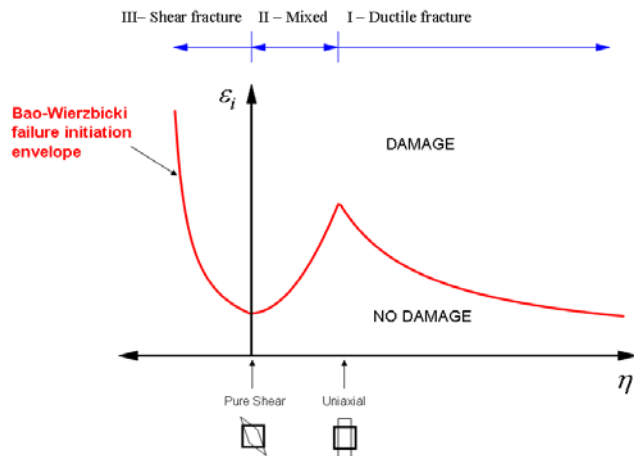


Figure 3: Schematic of Fracture Initiation Envelope Based on Stress Triaxiality

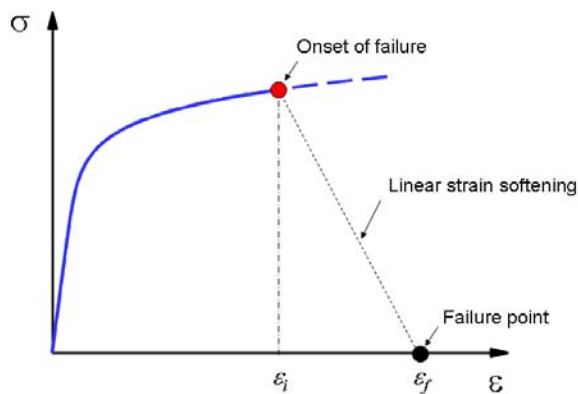


Figure 4: Schematic of Linear Strain Softening

The ABAQUS implementation of the B-W criterion was used to calculate the energy to fracture unnotched Charpy specimens made from TC-128B tank car steel under pendulum impact loading [17]. Results from the FEA simulations were in excellent agreement with the experimental data for the range of specimen thicknesses that were tested. Subsequently, this material failure methodology was used in conjunction with a Lagrangian fluid mesh formulation to predict puncture in a full-scale tank car shell impact test [6].

LS-DYNA Implementation

The finite element models used in the LS-DYNA simulations are developed using Altair’s software Hypermesh. All LS-DYNA simulations discussed in this paper are performed with Livermore Software Technology

Corporation’s (LSTC) LS-DYNA3D (version 970) [13], an explicit finite element solver for modeling impact.

The tank car container and jacket structure are modeled using shell elements. To minimize computational time, the FEA model of the tank consists of two parts: (1) a large area of rigid material away from the impacting end and, (2) a smaller area of deformable material at the impacting end, as illustrated in Figure 5. The model has boundary conditions similar to those used in ABAQUS simulations. Both Eulerian and Lagrangian fluid formulations are used in the modeling of fluid in LS-DYNA simulations.

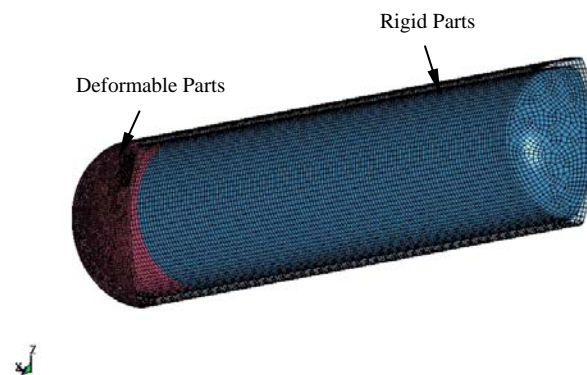


Figure 5: LS-DYNA Model of Rigid-Deformable Tank

The LS-DYNA FEA model with fluid-structure interaction uses Arbitrary-Lagrangian-Eulerian (ALE) coupling, which consists of four parts: (1) the tank structure (Lagrangian mesh), (2) an air block surrounding the tank structure (Eulerian mesh), (3) the liquid inside the tank (Eulerian mesh), and (4) the vapor outage that fills the remaining volume inside the tank (Eulerian mesh). In this context, a Lagrangian mesh is one that transforms according to its deformation; an Eulerian mesh is fixed in space through which material flows.

Material deformation for the fluid is characterized by a constitutive model called MAT_NULL with an equation of state, with a density of 0.051048 lbs/in³ and bulk modulus of 2.25 psi.

At present, LS-DYNA does not have a resident material model to implement the failure criterion described previously. Implementation of the B-W criterion can be performed through the user-defined material capability in LS-DYNA, but was conducted in this paper.

FEA RESULTS

The FEA models developed for railroad tank car head impacts are used to: (1) compare results from the two solvers with different formulations to account for fluid-structure interaction, (2) examine force-indentation behavior of different tank car configurations, and (3) predict puncture.

Comparison of Solvers and Fluid Formulations

Fluid-structure interaction is modeled in LS-DYNA using either a Lagrangian or an Eulerian mesh for the fluid. In ABAQUS, the fluid is modeled with a Lagrangian mesh. In both solvers, the tank structure is modeled with a Lagrangian mesh. In the previous work on tank car shell impacts [6], the LS-DYNA implementation of the Eulerian fluid provided excellent agreement with full-scale impact test data.

FEA results from ABAQUS and LS-DYNA with different fluid mesh formulations are shown in Figure 6. The tank car is traveling at 10 miles per hour (mph) in these simulations. The maximum impact forces are within 10 percent. Furthermore, these results show that there is no significant difference among the three models during the initial 0.05 second.

Figure 7 illustrates the corresponding force-indentation characteristics for these simulations. Indentation is measured from the initial position of the commodity tank. The figure indicates that all of the models are generally in good agreement, specifically the two models based on the Lagrangian fluid formulation. Differences are evident in the unloading portion of these curves that characterize the permanent deformation of the tank. However, the differences in permanent indentations are also within 10 percent. Maximum indentations are within 10 percent of each other.

Structural Response of Different Configurations

The force-indentation behavior of different tank car configurations is examined using LS-DYNA with an Eulerian mesh representing the fluid content inside the tank. The combination of LS-DYNA and Eulerian fluid mesh is chosen because the previous results with different solvers and fluid meshes showed no significant differences. In addition, the previous work using LS-DYNA with the Eulerian fluid mesh agreed well with full-scale shell impact test data [6].

Table 2 lists the three configurations considered in this paper. In general, the variables in these configurations are tank thickness, jacket thickness, and material (i.e., steel specification). In the configurations with head shields, the jacket in the head is replaced with a thicker sheet made of different steel. Varying these thicknesses also changes the gross weight of the tank car.

Figure 8 compares the force-time histories for these simulations. The peak impact forces increase as the tank head is thickened and head protection is added. The variation in peak forces among the three cases is approximately 20 percent.

Figure 9 shows the corresponding force-indentation curves. These curves have a nearly bi-linear character with a slightly higher breakpoint as additional layers of steel are added to the entire structure. This figure also indicates that adding thickness to the tank and providing a head shield decreases maximum indentation by as much as 23 percent.

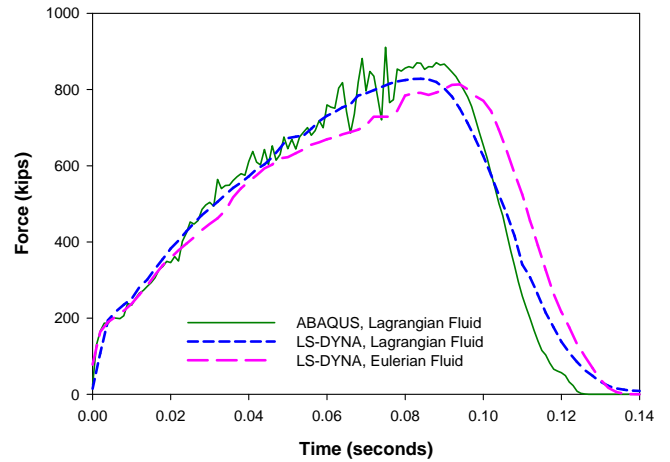


Figure 6: Force-Time Histories for Head Impact Simulations at 10 mph

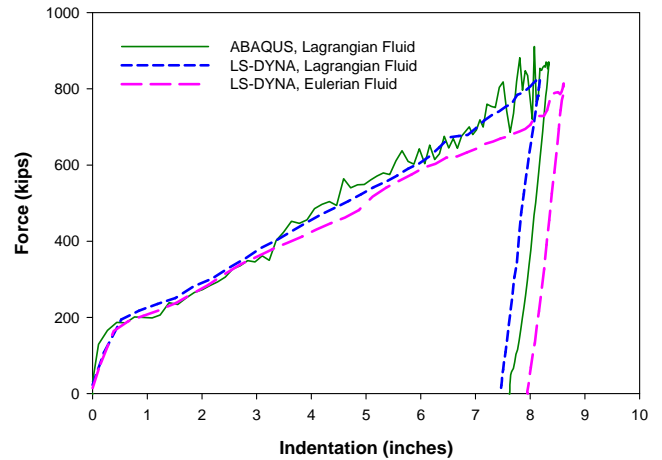


Figure 7: Force-Indentation Curves for Head Impact Simulations at 10 mph

Table 2: Characteristics of Tank Car Configurations

Configuration	1	2	3
	Baseline	Baseline with Head Shield	Thicker Baseline with Head Shield
Characteristic			
Inner Diameter (inch)	100.625	100.625	100.625
Weight (lb)	266,000	268,000	275,000
Tank Head Thickness (inch)	0.828	0.828	1.108
Tank Material	TC-128B	TC-128B	A516-70
Tank Shell Thickness (inch)	0.777	0.777	0.932
Tank Shell Material	TC-128B	TC-128B	TC-128B
Jacket Head Thickness (inch)	0.119	0.5	0.5
Jacket Head Material	A1011	A516-70	A516-70
Jacket Shell Thickness (inch)	0.119	0.119	0.119
Jacket Shell Material	A1011	A1011	A1011
Outage	10.6%	10.6%	10.6%
Internal Pressure (psi)	100	100	100

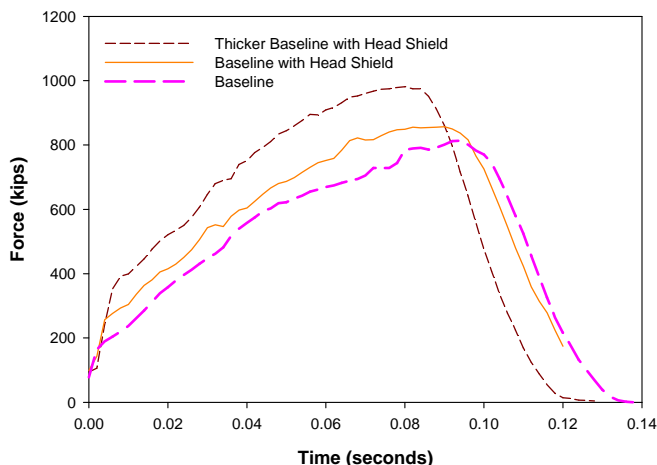


Figure 8: Simulated Force-Time Histories for 10-mph Head Impacts on Different Configurations

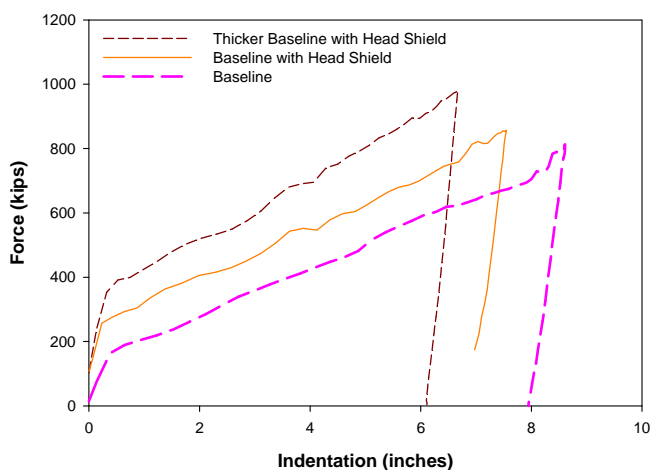


Figure 9: Simulated Force-Indentation Curves 10-mph Head Impacts on Different Configurations

The force-indentation behavior of different configurations is examined further by varying the impact speed. Table 3 compares the maximum forces for the different tank car configurations at three impact speeds between 10 and 15 mph. The numbers in parentheses refer to results from the semi-empirical method to calculate impact force as a function of velocity. Forces calculated with the semi-empirical method are generally higher than those from the FEA model. The one exception is the thicker baseline with head shield at 10 mph where the semi-empirical result is about 3 percent lower than the FEA calculation. Otherwise the semi-empirical results are between 7 and 33 percent higher than the FEA results. The differences in peak forces between the two methods become larger as impact velocity increases.

Table 3: Comparison of Maximum Force for Different Impact Speeds (kips)

Configuration	Speed of Moving Tank Car		
	10 mph	12.5 mph	15 mph
Baseline	813 (905)	984 (1265)	1248 (1663)
Baseline with Head Shield	857 (916)	1132 (1280)	1412 (1682)
Baseline with Increase Thickness and Head Shield	982 (952)	1254 (1330)	1562 (1748)

The impact scenario for which the semi-empirical method was developed is a moving ram car striking the head of a subject tank car below the centerline of the head. The impact location is assumed to be halfway between the centerline of the head and the bottom of the tank. The subject tank car with brakes released is braced by three fully-loaded backup or anvil cars with their brakes applied. Moreover, the generalized impact scenario examined by FEA in this paper is considered more severe than the one developed for the semi-empirical method. The equations comprising the semi-empirical method to calculate force, indentation, and puncture velocity for head impacts were originally reported in reference [8]. The modifications to include the presence of jackets and head shield are listed in reference [9]. In addition, the semi-empirical equations may also be found in reference [10].

Table 4 compares maximum indentations from the FEA simulations and the semi-empirical method. These results indicate that thickening the commodity tank and providing a head shield reduce maximum indentation. The table also indicates that the semi-empirical approach calculates maximum indentations that are between 40 and 70 percent less than those from the finite element method.

Table 4: Comparison of Maximum Indentation for Different Impact Speeds (inches)

Configuration	Speed of Moving Tank Car		
	10 mph	12.5 mph	15 mph
Baseline	8.6 (5.1)	10.8 (6.4)	12.9 (7.7)
Baseline with Head Shield	7.6 (3.1)	10.0 (3.9)	12.0 (4.6)
Baseline with Increase Thickness and Head Shield	6.6 (2.1)	9.0 (2.6)	11.1 (3.2)

Comparisons between the finite element and semi-empirical results show the conservative nature of the semi-empirical approach. However, while the semi-empirical method can provide reasonable estimates of peak impact force in some cases, it significantly underestimates maximum

indentation. The discrepancies between results from the FEA and the semi-empirical method may be attributed to differences in theoretical bases. The theoretical basis for the semi-empirical method is Hertz contact, which assumes quasi-static, elastic deformation of bodies in contact. Collisions that occur during accidents are likely to create permanent plastic deformations for which Hertz contact theory is not applicable.

Tank Car Head Puncture Predictions

Under relatively low initial impact velocities, the commodity tank may be permanently deformed but not punctured. As the impact velocity increases, the likelihood of puncture and consequent loss of structural integrity becomes greater. Therefore, a minimum initial impact velocity exists that first leads to puncture, which can be defined as a threshold puncture velocity. This threshold puncture velocity depends on factors such as impact mass, material, geometric and connectivity configurations of the tank car assembly (including type and outage amount of any fluid content), shape, size and location of the indenter, and all relevant initial and boundary conditions.

The ABAQUS model is exercised to predict puncture of railroad tank cars under head impacts. Particular focus is given to examine the effects of tank car thickness and indenter size. The three tank car configurations outlined in Table 2 are considered. Increased tank thicknesses in Configurations 2 and 3 lead to slightly higher collision mass compared to the Configuration 1. Being consistent with industrial applications, these two configurations also have different tank car steel materials in the head and/or the head jacket. The effect of indenter size is studied by considering both a 6-inch by 6-inch and a 12-inch by 12-inch indenter with a square-shaped face. The locations of the indenter centers relative to the tank car assembly are identical in the case studies.

The three tank car configurations and the two indenter sizes yield a maximum of six combinations for case studies. The model is exercised for five combinations without the combination of Configuration 3 and the larger size indenter. For each combination under consideration, finite element analyses incorporating the progressive damage and failure material models are conducted for initial impact velocities incremented at 1 mph. From the analyses, two impact velocities can be identified for each combination: (1) the highest velocity under which puncture is not clearly present (v_{np}), and (2) the lowest velocity under which puncture is clearly observed (v_p). The estimated threshold puncture velocities clearly lie between these two characteristic velocities.

Figure 10 shows four possible states of damage in the impacted region that develop on the commodity tank in the simulations, which help determine v_{np} and v_p . State (a) shows a permanently dented tank with surface damage. State (b) shows a more severely damaged tank where the local thickness has reduced significantly but shows no evidence of

through-the-thickness damage. State (c) shows obvious damage through the thickness. Finally, state (d) shows full penetration or puncture with or without turning part of the tank into a flap. Generally, v_{np} corresponds to initial impact velocities that lead to damage states (a) or (b), and v_p to those that lead to damage states (c) and (d). Special considerations are made for initial impact velocities leading to damage states (b) and (c) since these velocities appear to be extremely close to the threshold puncture velocity. For example, when v_{np} is determined according to damage state (b), the corresponding v_p is denoted as v_{np+} . When v_p is determined according to damage state (c), the corresponding v_{np} is denoted as v_{p-} .

The v_{np} and v_p results are tabulated in Table 5 for all five combinations denoted as Cases A through E. Identifying and categorizing damage states, particularly (b) and (c), can be subjective. Consequently, some numbers listed in Table 5 are changeable within their close neighborhoods. The table also includes predictions for puncture velocity based on the semi-empirical method. In general, the puncture velocities from the semi-empirical methods are less than those from the FEA for the same configuration and indenter size. Moreover, Table 5 indicates that increased tank car thicknesses and adding a head shield provide marginal or incremental improvements in the estimated threshold puncture velocities, and indenter size has a significant effect on the estimated puncture velocity.

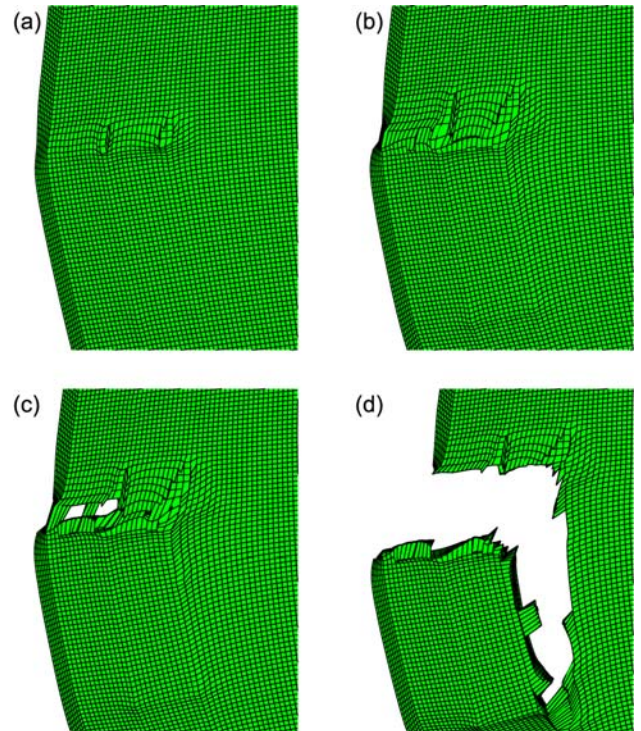


Figure 10: Potential Damage States of Impacted Region on Commodity Tank

Table 5: Puncture Velocity Estimation

Case	Configuration / Indenter size	FEA		Semi-Empirical
		v_{np} (mph)	v_p (mph)	v_p (mph)
A	Configuration 1 / 6-inch indenter	9	10	8.9
B	Configuration 2 / 6-inch indenter	10	11	10.3
C	Configuration 3 / 6-inch indenter	11	12	10.5
D	Configuration 1 / 12-inch indenter	16	16+	14.0
E	Configuration 2 / 12-inch indenter	16	17	16.3

Figure 11 shows the force-indentation curves obtained from the analyses for the five combinations, denoted as Cases A through E. The curve for each combination corresponds to an initial impact velocity that is closest to the estimated threshold puncture velocity. As shown in previous results, thickening the tank and providing a head shield tends to increase the impact force. Cases A and D correspond to the baseline tank car configuration with two indenter sizes. Similarly, Cases B and E correspond to the configuration for a baseline tank with head shield and different indenters. In both configurations, the force levels for the larger indenter are higher than those for the smaller indenter. For a given configuration, higher force levels associated with higher impact speeds are needed to puncture the tank with a larger indenter. In terms of energy to puncture, which is the area under the force-indentation curve, the larger indenter requires substantially more energy to puncture than the smaller indenter.

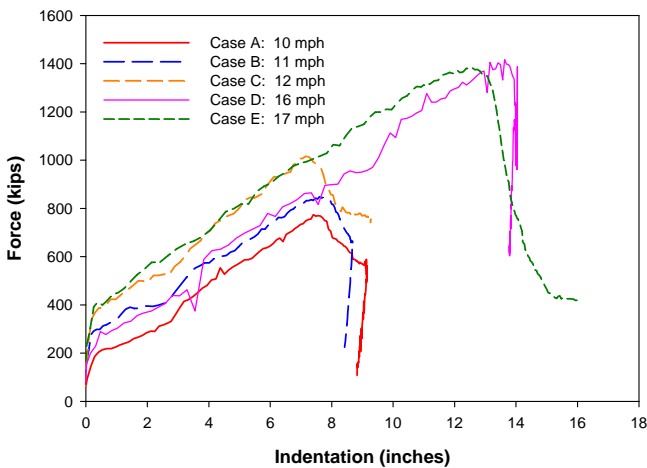


Figure 11: Force-Indentation Curves from Puncture Study

CONCLUDING REMARKS

Dynamic, nonlinear (i.e., elastic-plastic) finite element models have been developed to study the force-indentation behavior of railroad tank cars under head impact conditions. The models were developed using two commercial finite element codes, ABAQUS and LS-DYNA. These codes were used previously to develop a finite element framework to examine the structural behavior of tank cars under shell impacts [6, 7]. In this paper, the FEA framework was adapted to address head impacts in a consistent and analogous manner like shell impacts.

Different fluid mesh formulations were used to account for the effect of fluid-structure interaction in the FEA models. The models with different fluid mesh formulations were generally in agreement with each other.

The FEA models for head impacts were used to examine force-indentation behavior of different tank car configurations. These models showed that increasing the thickness of the head and adding a head shield tend to increase the maximum impact force while decreasing the maximum indentation.

Results from the FEA models for head impacts were compared to those from a semi-empirical method originally developed in the 1970s and subsequently modified to account for the presence of jackets and head shields. Peak impacts forces estimated from the semi-empirical method were generally higher than those from FEA. Conversely, maximum indentations calculated from the semi-empirical method were significantly less than those from FEA. Moreover, the comparisons suggest that the semi-empirical method provides reasonable but conservative estimates for peak impact force. Estimates for maximum indentation based on the semi-empirical method are significantly less than those from the FEA models.

The FEA models were also used to predict puncture of the tank car head. The results presented in this paper indicate that increasing the head thickness and adding a head shield provide marginal or incremental improvements in puncture velocity. The semi-empirical method generally predicts lower puncture velocities than the finite element method. The results also suggest that indenter size has a significant effect on the estimated puncture velocity. Moreover, the results presented in this paper are qualitatively and quantitatively consistent with FEA results previously conducted for shell impacts [7].

ACKNOWLEDGMENTS

The Federal Railroad Administration (FRA) Office of Research & Development sponsored the work described in this paper. Mr. Francisco Gonzalez is the FRA project manager for research on railroad tank cars. Mr. Eloy Martinez also provided technical direction to this project. Technical discussions with Professor A. Benjamin Perlman of the Volpe Center are greatly appreciated. Finally, the authors would like

to acknowledge Professor Christopher Barkan of the University of Illinois at Urbana-Champaign for his assistance in providing the Volpe Center with access to computers at the National Center for Supercomputing Applications.

REFERENCES

- [1] National Transportation Safety Board, 2004: "Derailment of Canadian Pacific Railway Freight Train 292-16 and Subsequent Release of Anhydrous Ammonia Near Minot, North Dakota January 18, 2002," Railroad Accident Report NTSB/RAR-04/01.
- [2] National Transportation Safety Board, 2005: "Collision of Norfolk Southern Freight Train 192 With Standing Norfolk Southern Local Train P22 With Subsequent Hazardous Materials Release at Graniteville, South Carolina January 6, 2005," Railroad Accident Report NTSB/RAR-05/04.
- [3] National Transportation Safety Board, 2006: "Collision of Union Pacific Railroad Train MHOTU-23 With BNSF Railway Company Train MEAP-TUL-126-D With Subsequent Derailment and Hazardous Materials Release, Macdona, Texas, June 28, 2004," Railroad Accident Report NTSB/RAR-06/03.
- [4] Tyrell, D.C., Jeong, D.Y., Jacobsen, K., Martinez, E., 2007: "Improved Tank Car Safety Research," *Proceedings of 2007 ASME Rail Transportation Division Fall Technical Conference*, RTDF2007-46013.
- [5] Jeong, D.Y., Tang, Y.H., Yu, H., Perlman, A.B., 2006: "Engineering Analyses for Railroad Tank Car Head Puncture," *Proceedings of IMECE2006*, 2006 ASEM International Mechanical Engineering Congress and Exposition, IMECE2006-13212.
- [6] Tang, Y.H., Yu, H., Gordon, J.E., Priante, M., Jeong, D.Y., Tyrell, D.C., Perlman, A.B., 2007: "Analysis of Full-Scale Tank Car Shell Impact Tests," *Proceedings of 2007 ASME Rail Transportation Division Fall Technical Conference*, RTDF2007-46010.
- [7] Tang, Y.H., Yu, H., Gordon, J.E., Jeong, D.Y., 2008: "Analysis of Railroad Tank Car Shell Impacts Using Finite Element Method," *Proceedings of the 2008 IEEE/ASME Joint Rail Conference*, JRC2008-63014.
- [8] Shang, J.C., Everett, J.E., 1972: "Impact Vulnerability of Tank Car Heads," *Shock and Vibration Bulletin* 42, 197-210.
- [9] Belpoort, S.M., 1993: "Evaluation of the Puncture Resistance of Stainless Steel and Carbon Steel Tank Heads," AAR Report No. P-93-114.
- [10] Jeong, D.Y., Tang, Y.H., Perlman, A.B., 2001: "Evaluation of Semi-Empirical Analyses for Railroad Tank Car Puncture Velocity, Part I: Correlations with Experimental Data," Volpe Center Report, DOT/FRA/ORD-01/21.1.
- [11] Jeong, D.Y., Tang, Y.H., Perlman, A.B., 2001: "Evaluation of Semi-Empirical Analyses for Railroad Tank Car Puncture Velocity, Part II: Comparisons with Engineering Analyses," Volpe Center Report, DOT/FRA/ORD-01/21.2.
- [12] *ABAQUS User's Manual*, Hibbit, Karlsson & Sorensen Inc., Pawtucket, Rhode Island.
- [13] *LS-DYNA3D User's Manual*, Version 970, Livermore Software Technology Company, Livermore, California.
- [14] American Society of Mechanical Engineers, 2006: "Guide for Verification and Validation in Computational Solid Mechanics," ASME V&V 10-2006, New York, NY.
- [15] Joia, C.J.B., Carneval, R.O., Soares, S.D., Bezerra, P.S.A., Azevedo, C., Cardoso, E.M., Mattos, O.R., Menendez, C.M., 2000: "Monitoring hydrogen damage in pipelines and pressure vessels," Corrosion 2000, Paper No. 469, NACE International, Houston, Texas.
- [16] Bao, Y., Wierzbicki, T., 2004: "On fracture locus in the equivalent strain and stress triaxiality space," *International Journal of Mechanical Sciences* 46, 81-98.
- [17] Yu, H., Jeong, D.Y., Gordon, J.E., Tang, Y.H., 2007: "Analysis of Impact Energy to Fracture Unnotched Charpy Specimens Made from Railroad Tank Car Steel," *Proceedings of the 2007 ASME Rail Transportation Division Fall Technical Conference*, RDTF2007-46038.